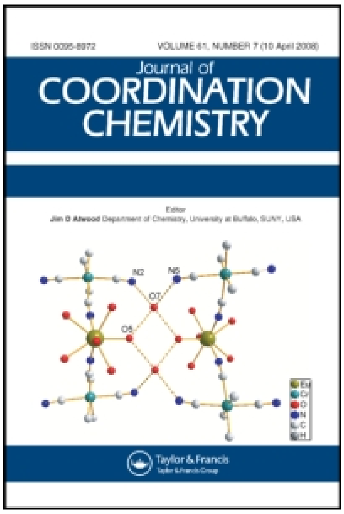

Journal of Coordination Chemistry
Publication details, including instructions for authors and subscription information:
http://www.informaworld.com/smpp/title~content=t713455674

Thermodynamics of Formation of Ru(III) and Ru(IV)-µ-Peroxo Complexes

M. M. Taqui Khan[a]; M. A. Moiz[a]; Amjad Hussain[a]
[a] Discipline of Coordination Chemistry and Homogeneous Catalysis, Central Salt and Marine Chemicals Research Institute, Bhavnagar, India

To cite this Article Khan, M. M. Taqui , Moiz, M. A. and Hussain, Amjad(1991) 'Thermodynamics of Formation of Ru(III) and Ru(IV)-µ-Peroxo Complexes', Journal of Coordination Chemistry, 23: 1, 245 — 256
To link to this Article: DOI: 10.1080/00958979109408255
URL: http://dx.doi.org/10.1080/00958979109408255

J. Coord. Chem. 1991, Vol. 23. pp. 245–256
Reprints available directly from the publisher
Photocopying permitted by license only

THERMODYNAMICS OF FORMATION OF Ru(III) AND Ru(IV)-μ-PEROXO COMPLEXES*

M. M. TAQUI KHAN,† M. A. MOIZ, and AMJAD HUSSAIN

Discipline of Coordination Chemistry and Homogeneous Catalysis, Central Salt and Marine Chemicals Research Institute, Bhavnagar 364 002, India

(Received June 27, 1990; in final form December 12, 1990)

Reaction of one half and one equivalents of H_2O_2 with $K[Ru^{III}(pdta\text{-}H)Cl].2H_2O$ gives rise to the μ-peroxo complexes $[Ru^{III}(pdta\text{-}H)]_2H_2O_2$ and $[Ru^{IV}(pdta\text{-}H)]_2O_2$, respectively. Equilibrium constants for the formation of the various peroxo species were determined between pH 3–11, in the temperature range 283–313 K and with $\mu = 0.10$ M in KCl. The existence of the various peroxo species was substantiated by potentiometry, spectrophotometry and electrochemical studies. Thermodynamic quantities associated with the formation of the $(pdta)Ru^{III}$ and $(pdta)Ru^{IV}$-μ-peroxo species and their hydrolysis products are reported.

Keywords: Ruthenium, pdta, peroxo complexes, formation constants, thermodynamics

INTRODUCTION

Metal complexes containing peroxide or superoxide ligands are of biochemical significance as potential model systems for enzymes for the catalysis of the oxidation of organic compounds.[1] We have reported[2] earlier the reversible binding of dioxygen to Ru(III)-aminopolycarboxylates to form μ-peroxo-μ-hydroxo-Ru(IV) complexes. Equilibrium studies on the interaction of $K[Ru(edta\text{-}H)Cl].2H_2O$ with O_2 and H_2O_2 to form μ-peroxo complexes were also reported.[3] In order to study the effect of the basicity of the ligand on peroxo complex stability, we have studied the interaction of $K[Ru(pdta\text{-}H)Cl].2H_2O$ with one half and one equivalents of H_2O_2 to form μ-peroxo ruthenium(III) and (IV) complexes respectively. The reactions were studied in the pH range 3–11, in the temperature range 283–313 K and with $\mu = 0.1$ M (KCl). Thermodynamic parameters for the formation of the various species present in solution in the above mentioned pH range are also reported.

EXPERIMENTAL

Materials

Hydrated ruthenium chloride, $RuCl_3.xH_2O$, was obtained from Johnson Matthey; propylenedinitrilotetraacetic acid (PDTA) was purchased from Aldrich Chemical Co. and H_2O_2 (30%) was obtained from BDH Chemicals. All other reagents used were of A.R. grade. The nitrogen used was of analar grade (4 PPM O_2) and was

---

* Dedicated to Prof. A.E. Martell on the occasion of his 75th birthday.

† Author for correspondence.

purified by passing it through vanadous sulphate and alkaline pyrogallate solutions. $K[Ru(edta\text{-}H)Cl].2H_2O$, **1** and $K[Ru(pdta\text{-}H)Cl].2H_2O$, **2** were prepared by known procedures[3] and characterized by elemental analysis.

Physical measurements

All potentiometric titrations were performed using a Metrohm 682 Titroprocessor at four temperatures: 283, 293, 303 and 313K. The other conditions were the same as described previously.[3] DPP and CV were recorded on a PAR 174 electrochemical system, equipped with a Precision X-Y recorder and Model 173 galvanostat as described previously.[3] The electronic absorption spectra were recorded on a Shimadzu UV-160 spectrophotometer equipped with a TCC-240A temperature controller. Matched 10 or 2 mm quartz cuvettes were used. The spectra were recorded at 283, 293, 303 and 313K and with $\mu = 0.10$ M (KCl) against a reference 0.10 M KCl solution. Protonation constants and formation constants were computed by a curve-fitting method using the programs PKAS and BEST,[4] respectively.

RESULTS AND DISCUSSION

On dissolution of the complex $[Ru(pdta\text{-}H)Cl]^-$, **2** in water, Cl^- is immediately replaced by a water molecule[5] to form the aquo complex $[Ru(pdta\text{-}H)H_2O]$, **2a**. In all the reactions discussed subsequently, complex **2a** is taken as the complex species present in solution.

Potentiometry of complex 2a under N_2

The titration curve of complex **2a** under N_2 (Fig. 1a) shows two inflections at a = 1.0 and 2.0. The equilibria assumed in the buffer region between a = 0–1 and 1–2 are as follows,

$$\underset{\textbf{2a}}{M^{III}HL(H_2O)} \overset{K_1}{\rightleftharpoons} \underset{\textbf{2b}}{M^{III}L(H_2O)} + H^+$$

$$K_1 = [ML(H_2O)][H^+]/[MHL(H_2O)] \qquad (1)$$

$$\underset{\textbf{2b}}{M^{III}L(H_2O)} \overset{K_2}{\rightleftharpoons} \underset{\textbf{2c}}{M^{III}L(OH)} + H^+$$

$$K_2 = [ML(OH)][H^+]/[ML(H_2O)] \qquad (2)$$

where MHL denotes the complex $[Ru(pdta\text{-}H)H_2O]$, **2a**.

The complex **2c** does not show any further hydrolysis after a = 2.0. The constants log K_1 and log K_2 calculated at 303 K ($\mu = 0.10$ M KCl) by the program PKAS are tabulated in Table I. The reactions are shown in Scheme 1.

SCHEME-1

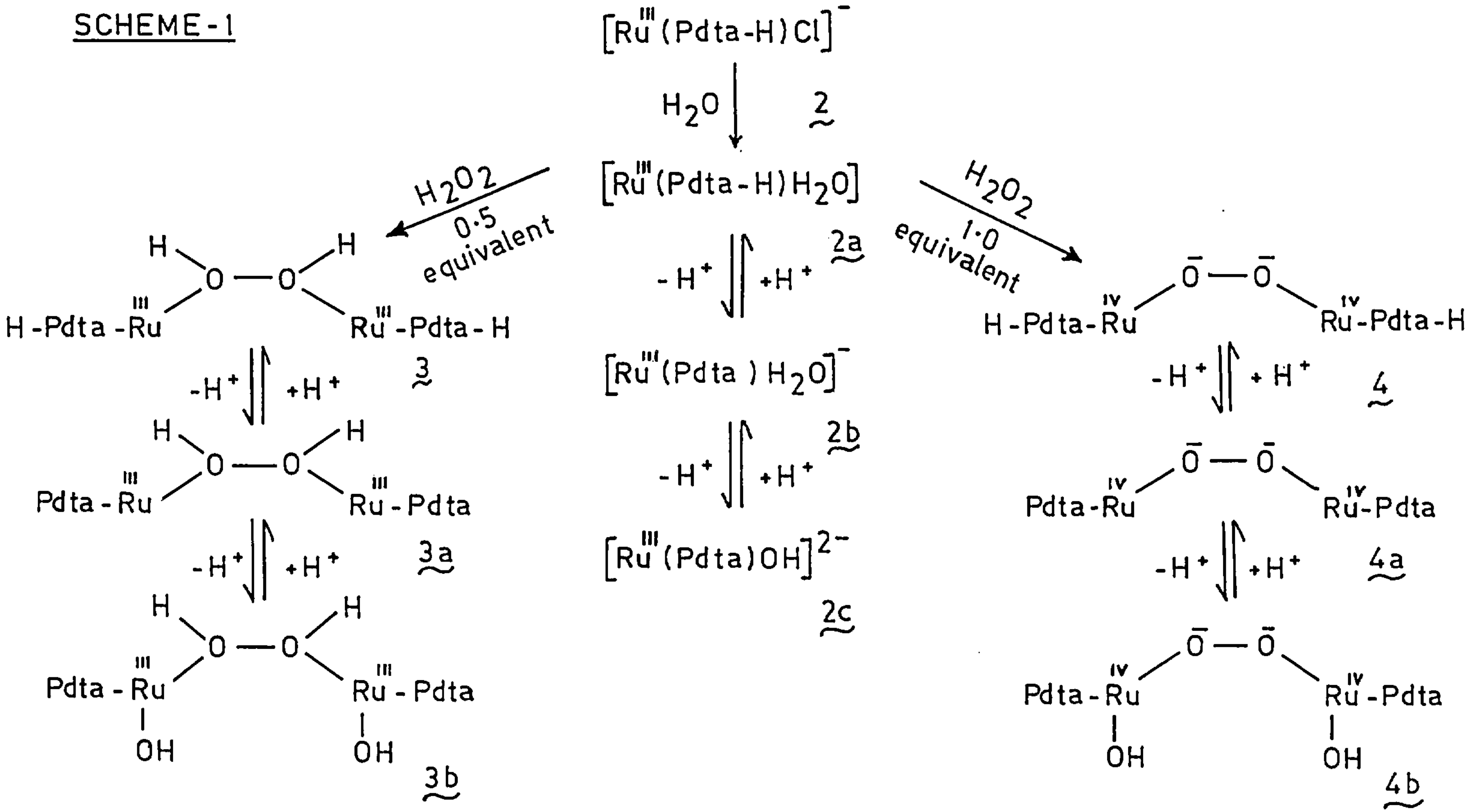
$[Ru^{III}(Pdta\text{-}H)Cl]^-$
H_2O
2
$[Ru^{III}(Pdta\text{-}H)H_2O]$
2a
$[Ru^{III}(Pdta)H_2O]^-$
2b
$[Ru^{III}(Pdta)OH]^{2-}$
2c
$-H^+$
$+H^+$
H_2O_2
0·5
equivalent
1·0
equivalent
H-Pdta-Ru
Ru-Pdta-H
Pdta-Ru
Ru-Pdta
OH
III
IV
3
3a
3b
4
4a
4b

TABLE I

Equilibrium and thermodynamic data for the complexes [Ru(edta-H)H_2O] and [Ru(pdta-H)H_2O] in the presence of N_2, half and one equivalents of H_2O_2, $\mu = 0.10$ M KCl.

Constants	Equilibrium Quotient	Complex	Log of equilibrium constant at 303 K	ΔH°/ kcal/mol	ΔS°/ cal/deg/mol	ΔG°/ kcal/mol
K_1	$[M^{III}L][H^+]/[M^{III}HL]$	EDTA	−2.53	13.3	32.0	3.5
		PDTA	−2.30	14.0	36.0	3.2
K_2	$[M^{III}L(OH)][H^+]/[M^{III}L]$	EDTA	−8.01	11.6	2.0	11.1
		PDTA	−8.17	10.0	−3.0	11.0
$K_{2'}$	$[M^{III}(OH)_2][H^+]/[M^{III}L(OH)]$	EDTA	−11.00	17.6	7.0	15.5
K_3	$[(M^{III}HL)_2H_2O_2]/[M^{III}HL]^2[H_2O_2]$	EDTA	9.40*	−34.9	−72.0	−13.0
		PDTA	10.00*	−36.5	−75.0	−13.8
K_4	$[(M^{III}L)_2H_2O_2][H^+]^2/[(M^{III}HL)_2H_2O_2]$	EDTA	−3.24	−13.7	−60.0	4.5
		PDTA	−3.05	−13.5	−58.0	3.9
K_5	$[(M^{III}L(OH)_2H_2O_2][H^+]^2/[(M^{III}L)_2H_2O_2]$	EDTA	−8.88	−12.6	−82.0	12.3
		PDTA	−9.05	−11.5	−80.0	12.2
$K_{5'}$	$[(M^{III}L(OH)_2)_2H_2O_2][H^+]^2/[(M^{III}L(OH))_2H_2O_2]$	EDTA	−10.96	−23.5	−127.0	15.2
K_6	$[(M^{IV}HL)_2O_2]/[(M^{III}HL)]^2[H_2O_2]^2$	EDTA	11.45*	−37.4	−71.0	−15.9
		PDTA	11.75*	−39.2	−76.0	−16.6
K_7	$[(M^{IV}L)_2O_2][H^+]^2/[(M^{IV}HL)_2O_2]$	EDTA	−2.75	−9.5	−44.0	3.8
		PDTA	−2.55	−9.2	−42.0	3.3
K_8	$[(M^{IV}L(OH))_2O_2][H^+]^2/[(M^{IV}L)_2O_2]$	EDTA	−9.24	−8.7	−71.0	12.8
		PDTA	−9.30	−8.4	−71.0	12.6
$K_{8'}$	$[(M^{IV}L(OH)_2)_2O_2][H^+]^2/[(M^{IV}L(OH))_2O_2]$	EDTA	−10.88	−14.3	−97.0	15.1

* By spectrophotometry.

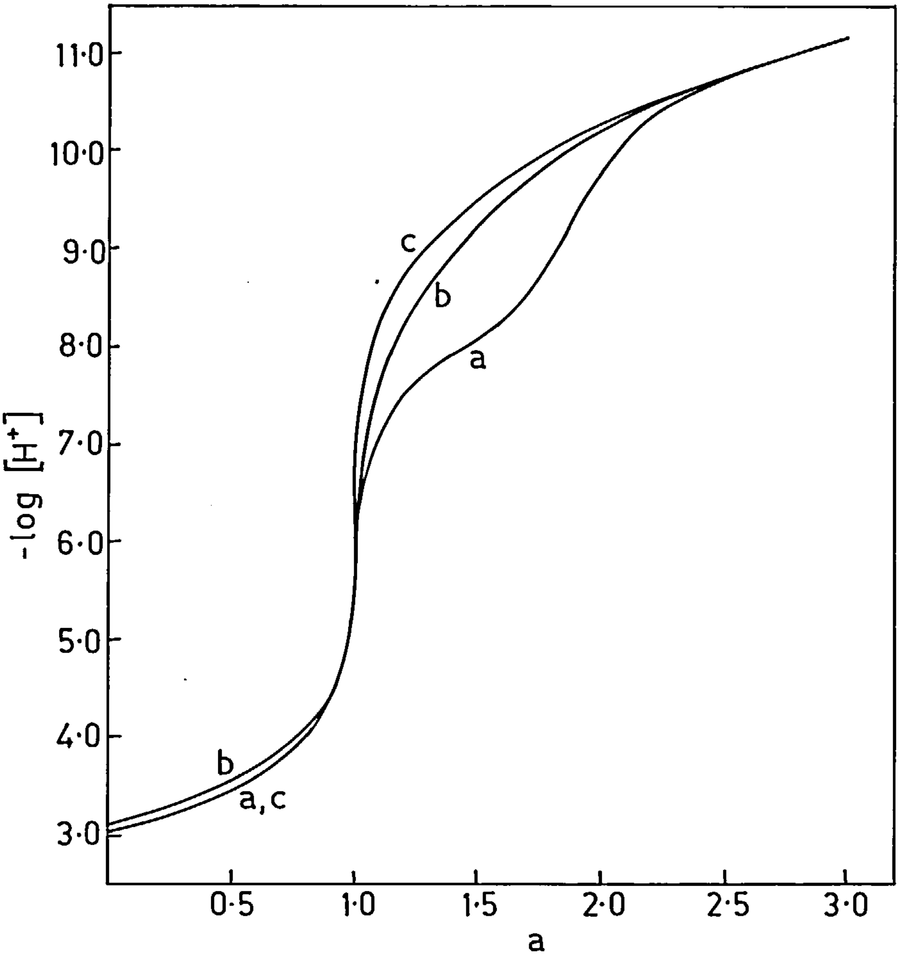

FIGURE 1 Potentiometric titration curves of [Ru(pdta-H)H_2O] (1×10^{-3} M) solutions at 303K and with $\mu = 0.1$ M KCl (a): under N_2; (b): in the presence of 0.5 equivalents of H_2O_2; (c): in the presence of 1.0 equivalents of H_2O_2.

The crystal structure[6] of complex **2** shows that PDTA acts as a pentadentate ligand with Cl^- occupying the sixth coordination position. The proton on the uncoordinated carboxylic acid group in complex **2a** is neutralized between a = 0–1 to give complex **2b**. The hydrolysis of complex **2b** between a = 1–2 is due to deprotonation of the water molecule already coordinated to Ru(III) to give complex **2c**. The dissociation constant of complex **2a** is lower than with the [Ru(edta-H)H_2O] complex **1a**.[3] This is due to the presence of the electron donating CH_3 group in complex **2a**.

Potentiometry of complex 2a in the presence of 0.5 equivalents of H_2O_2

The potentiometric titration curve of complex **2a** in the presence of 0.5 equivalents of H_2O_2 is shown in Fig. 1b. The curve shows a steep inflection at a = 1.0 and lies above the titration curve of the 1.0 equivalent H_2O_2 system (Fig. 1c). In the buffer region between a = 0–1 plausible reactions are as follows;

$$\underset{\mathbf{2a}}{2M^{III}HL(H_2O)} + H_2O_2 \overset{K_3}{\rightleftharpoons} \underset{\mathbf{3}}{(M^{III}HL)_2H_2O_2} + 2H_2O$$

$$K_3 = [(M^{III}HL)_2H_2O_2]/[M^{III}HL(H_2O)]^2[H_2O_2] \qquad (3)$$

$$\underset{\mathbf{3}}{(M^{III}HL)_2H_2O_2} \overset{K_4}{\rightleftharpoons} \underset{\mathbf{3a}}{(M^{III}L)_2H_2O_2} + 2H^+$$

$$K_4 = [(M^{III}L)_2H_2O_2][H^+]^2/[(M^{III}HL)_2H_2O_2] \qquad (4)$$

The constants log K_3 and log K_4 are given in Table I.

The buffer region between a = 1–2 (Fig. 1b) lies above the corresponding buffer region under N_2 and does not show any inflection beyond a = 1.0. The 1 : 0.5 H_2O_2 curve lies below that of the 1:1 H_2O_2 curve (Fig. 1c). The following reaction is assumed to take place in the buffer region between a = 1–2.

$$\underset{\mathbf{3a}}{(M^{III}L)_2H_2O_2} + 2H_2O \overset{K_5}{\rightleftharpoons} \underset{\mathbf{3b}}{(M^{III}L(OH))_2H_2O_2} + 2H^+$$

$$K_5 = [(M^{III}L(OH))_2H_2O_2][H^+]^2/[(M^{III}L)_2H_2O_2] \qquad (5)$$

The constant corresponding to equation (*5*) is also given in Table I. Reactions are shown in Scheme I.

Potentiometry of complex 2a in the presence of 1.0 equivalents of H_2O_2

The titration curve in the presence of 1.0 equivalents of H_2O_2 (Fig. 1c) shows a sharp inflection at a = 1.0, indicating the dissociation of a proton from the carboxyl group of complex **4** to give complex **4a**. The titration curve (Fig. 1c) overlaps with the curve (Fig. 1a); under N_2). This shows that there is no liberation of protons when complex **2a** reacts with 1.0 equivalents of H_2O_2 (equation *6*) and Ru(III) is oxidized to Ru(IV).

$$\underset{\mathbf{2a}}{2M^{III}HL} + 2H_2O_2 \overset{K_6}{\rightleftharpoons} \underset{\mathbf{4}}{(M^{IV}HL)_2O_2} + 2H_2O$$

$$K_6 = [(M^{IV}HL)_2O_2]/[M^{III}HL]^2[H_2O_2]^2 \qquad (6)$$

$$\underset{\mathbf{4}}{(M^{IV}HL)_2O_2} \overset{K_7}{\rightleftharpoons} \underset{\mathbf{4a}}{(M^{IV}L)_2O_2} + 2H^+$$

$$K_7 = [(M^{IV}L)_2O_2][H^+]^2/[(M^{IV}HL)_2O_2] \qquad (7)$$

Reactions (*6*) and (*7*) were assumed to take place in the buffer region a = 0–1. The constants corresponding to equation (*6*) calculated by a spectrophotometric method and equation (*7*) by an algebraic method are given in Table I. The buffer region between a = 1–2 (Fig. 1c) lies above those under N_2 and 1:0.5 H_2O_2 systems. A plausible reaction in this buffer region is as follows.

$$\underset{\mathbf{4a}}{(M^{IV}L)_2O_2} + 2H_2O \overset{K_8}{\rightleftharpoons} \underset{\mathbf{4b}}{(M^{IV}L(OH))_2O_2} + 2H^+$$

$$K_8 = [(M^{IV}L(OH))_2O_2][H^+]^2/[(M^{IV}L)_2O_2] \qquad (8)$$

The species **4b** does not show any further hydrolysis after a = 2.0. The constant corresponding to equilibrium (*8*) is given in Table I. Reactions are shown in Scheme I.

Electrochemical Studies

Electrochemical responses at dme of complex **2a** were recorded under N_2 in the presence of 0.5 and 1.0 equivalents of H_2O_2. The solutions prepared at a = 0.5, 1.5 and 2.5 are solution A, solution B and solution C, respectively. The electrochemical studies on solutions corresponding to Fig. 1a (under N_2) are A1, B1 and C1, to Fig. 1b (in the presence of 0.5 equivalents of H_2O_2), A2, B2 and C2 and to Fig. 1c (in the presence of 1.0 equivalents of H_2O_2), A3, B3 and C3, respectively. Fig. 2 shows the DPP and CV of solutions B1, B2 and B3. The reduction potentials ($E_{1/2}$) measured as the peak potentials in differential pulse polarograms (DPP) and cyclic voltammograms (CV) are given in Table II.

The DPP of solution A1 containing the species **2a** and **2b** at equilibrium exhibits two reduction steps at −0.25 and −0.83 V corresponding to the one-electron reduction of Ru^{3+}/Ru^{2+} [7] and $H^+/\frac{1}{2}H_2$ respectively. Solutions B1 and C1 exhibit only one peak corresponding to the Ru^{3+}/Ru^{2+} redox couple, with a shift in potential to more negative values. The cathodic shift in $E_{1/2}$ of Ru^{3+}/Ru^{2+} couple is due to the formation of the monohydroxo species **2c**. The CV of solutions A1, B1 and C1 (Table II) agree with the DPP results. The potentials at −0.225 V (0.5 (Epa + Epc)) correspond to the Ru^{3+}/Ru^{2+} redox couple. The proton reduction couple observed at −0.83 V in DPP is also observed in CV at −Epc = 0.89 V as an irreversible peak.

The DPP of solution A2 shows behaviour similar (Table II) to that of solution A1. Therefore it may be inferred that oxidation state of Ru in the presence of one half equivalent of H_2O_2 does not change. Thus ruthenium is in the +3 state in complex **3**. The CV of solution A2 shows cathodic and corresponding anodic peaks at −0.27 and −0.19 V, respectively, due to Ru^{3+}/Ru^{2+} reduction. Two small peaks at −0.51 and −0.67 V are also observed in the CV. These are due to reduction of the coordinated hydroperoxo group. These peaks are not exhibited in the CV at slow scan rates. This is due to the reduction of Ru^{3+} to Ru^{2+} at a slow scan rate and the subsequent decomposition of the dimer. Successive scans do not show these peaks and the CV resembles that of solution A1.

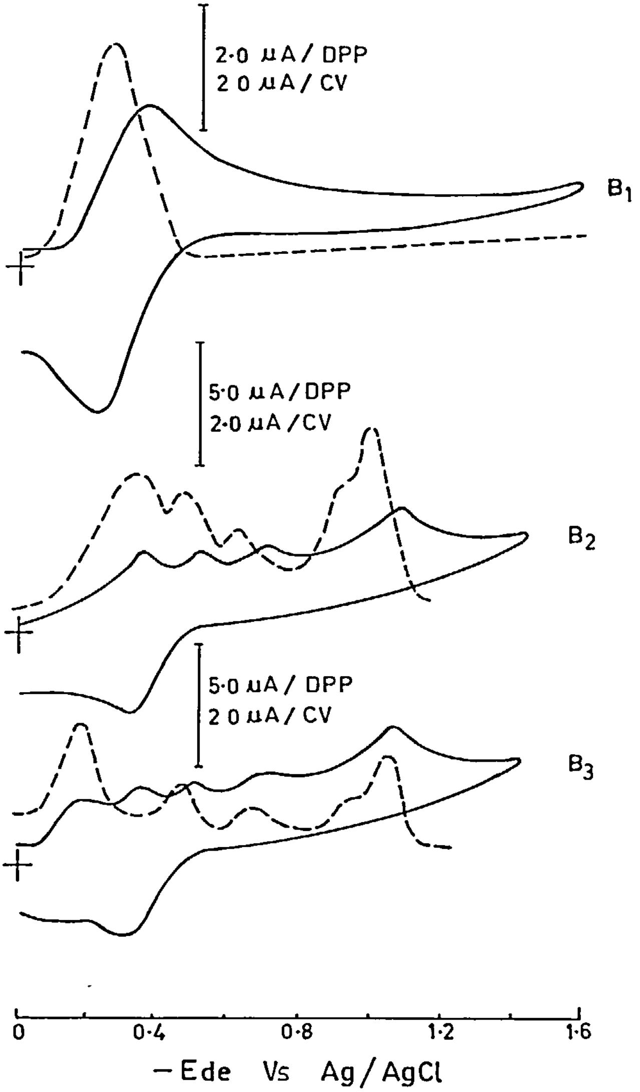

FIGURE 2 Differential pulse and cyclic voltammograms of [Ru(pdta-H)]H_2O (1 × 10^{-3} M) solutions at 303K and with $\mu = 0.1$ M KCl: (B1): at "a" ([NaOH]/[ML]) = 1.5 under N_2; (B2): at "a" ([NaOH]/[ML]) = 1.5 in the presence of 0.5 equivalents of H_2O_2; (B3): at "a" ([NaOH]/[ML]) = 1.5 in the presence of 1.0 equivalents of H_2O_2.

The DPP of solution B2 shows peaks at −0.34 V which is assigned to Ru^{3+}/Ru^{2+} as explained above. Unlike the DPP of solution A2, the DPP of solution B2 shows peaks due to reduction of the coordinated hydroperoxo group. The reason for this is the higher negative charge on **3a** as compared to **3** resulting in a stronger Ru^{III}–H_2O_2 bond. These peaks are also exhibited in the CV even at lower scan rates, thus showing the higher stability of **3a** with respect to **3**. However, successive scans do not exhibit these peaks and the CV again resembles that of solution B1. The CV of solution B2 shows cathodic and anodic peaks at −0.36 and −0.31 V respectively. This is assigned to Ru^{3+}/Ru^{2+} couple. The DPP and CV of solution C2 resembles that of solution B2 except that peaks are shifted to more negative potentials.

The DPP of solution A3 shows peaks at −0.20 and −0.85 V along with small peaks at −0.48 and −0.70 V. The peak at −0.20 V is assigned to the reduction of Ru^{4+}. This assignment is based on comparison of the DPP of $[(edta)Ru^{IV})_2O]^{2-}$ at pH 3.0[8] which exhibits a peak at −0.16 V, corresponding to the Ru^{4+}/Ru^{3+} couple. Peaks at −0.48 and −0.70 V are assigned to reduction of the μ-peroxo group. The CV of solution A3 gives an $E_{1/2}$ for the Ru^{4+}/Ru^{3+} couple of −0.23 V. Irreversible cathodic peaks at −0.50 and −0.67 V are assigned to reduction of the coordinated peroxo group. The DPP and CV of solution B3 is similar to that of A3 with a small positive shift in potential for the Ru^{4+}/Ru^{3+} couple (Table II). This is due to the presence of the hydroxo group.

TABLE II

Polarographic and cyclic voltammetric data for the complex $[Ru(pdta\text{-}H)H_2O]$ at different "a" ([NaOH]/[ML]) values; T = 303K, μ = 0.10 M (KCl).[b]

		DPP	CV	
Conditions	"a"	$-E_{1/2}$ V *vs* Ag/AgCl	−Epc V	−Epa V
N_2	0.5	0.25, 0.83	0.27, 0.89	0.18
	1.5	0.33	0.40	0.20
	2.5	0.37	0.45	0.29
H_2O_2	0.5	0.25, 0.83	0.27, (0.51), (0.67), 0.98	0.19
(1 : 0.5)[a]	1.5	0.34, 0.45, 0.63, 0.94, 1.03	0.36, 0.51, 0.67, 1.08	0.31
	2.5	0.40, 0.48, 0.69, 1.00, 1.10	0.40, 0.55, 0.70, 1.10	0.36
H_2O_2	0.5	0.20, (0.48), (0.70), 0.85	0.27, 0.50, 0.67, 0.88	0.19
(1 : 1)[a]	1.5	0.17, 0.47, 0.65, 0.94, 1.04	0.18, 0.50, 0.67, 0.97, 1.08	0.30
	2.5	0.15, 0.43, 0.64, 0.97, 1.06	0.17, 0.43, 0.63, 0.99, 1.11	0.38

[a] Ratio of complex to H_2O_2. [b] Values shown in parentheses refer to peak potentials for low peak currents.

Spectrophotometry

In order to substantiate the conclusions derived from potentiometric and electrochemical results, the solutions A1, B1 and C1, solutions A2, B2 and C2 and solutions A3, B3 and C3 were studied spectrophotometrically. The spectral data are presented in Table III. Solution A1 under nitrogen exhibits two shoulders at 240 nm (ε 3.32 × 10^3)* and 282 nm (ε 2.48 × 10^3) which may be assigned to charge transfer (CT) bands of pdta. In addition to these, the spectrum shows a broad shoulder at 371 nm (ε 5.35 × 10^2). This may be due to metal-aquo/OH^- coordination. Solutions B1 and C1 show the same bands with a decrease in intensity.

Solution A2 in the presence of 0.5 equivalents of H_2O_2 shows two bands at 208 nm (ε 1.03 × 10^4) and 393 nm (ε 7.65 × 10^3) and a shoulder at 307 nm (ε 2.50 × 10^3). The band at 208 nm may be assigned to the CT band of pdta and the bands at 307 nm and 393 nm may be assigned[9] to $1\pi^*h(H_2O_2) \rightarrow Ru(III)$ and $1\pi^*y(H_2O_2) \rightarrow Ru(III)$

---

* $M^{-1}\,cm^{-1}$.

respectively. Similar bands were observed in the μ-hydroperoxo complex of edta. The spectra of solution B2 and C2 are similar to the spectrum of solution A2 indicating that the μ-hydroperoxo complex is quite stable and does not decompose on increasing pH with subsequent hydrolysis of the metal ion.

Solution A3 in the presence of 1.0 equivalents of H_2O_2 exhibits four bands at 208 nm (ε 1.20 × 10^4), 307 nm (ε 2.56 × 10^3), 393 nm (ε 7.82 × 10^3) and 632 nm (ε 1.72 × 10^2). That at 632 nm may be assigned to a Ru(IV) $\rightarrow O_2^{2-}$ MLCT[9] band. A similar band was observed[3] in the μ-peroxo complex of Ru(IV)-edta. The shoulder at 307 nm and a band at 393 nm are the LMCT bands and may be assigned to the $1\pi^*$ component of the LMCT of monobridged coordinated peroxoRu(IV). The band at 208 nm is the CT band of pdta. Solutions B3 and C3 also exhibit these peaks, with almost the same intensities, thus indicating the formation of very stable μ-peroxo complexes of Ru(IV)-pdta.

TABLE III

Absorption spectral data for the complex [Ru(pdta-H)H_2O] at different "a" ([NaOH]/[ML]) values; T = 303K; μ = 0.10 M KCl.

Conditions	λ_{max}, nm (ε, M^{-1} cm^{-1})		
	Solution A	Solution B	Solution C
	a = 0.5	a = 1.5	a = 2.5
N_2	240_{sh} (3.32 × 10^3)	240_{sh} (3.94 × 10^3)	240_{sh} (4.00 × 10^3)
	282_{sh} (2.50 × 10^3)	282_{sh} (2.29 × 10^3)	285_{sh} (2.10 × 10^3)
	371_{wsh} (5.35 × 10^2)	371_{wsh} (5.05 × 10^2)	371_{wsh} (4.80 × 10^2)
H_2O_2 (1 : 0.5)[a]	208_{vs} (1.03 × 10^4)	208_{vs} (1.03 × 10^4)	208_{vs} (1.03 × 10^4)
	307_{sh} (2.50 × 10^3)	307_{sh} (2.45 × 10^3)	307_{sh} (2.40 × 10^3)
	393_{vs} (7.65 × 10^3)	393_{vs} (7.52 × 10^3)	393_{vs} (7.43 × 10^3)
H_2O_2 (1 : 1)[a]	208_{vs} (1.03 × 10^4)	208_{vs} (1.03 × 10^4)	208_{vs} (1.03 × 10^4)
	307_{sh} (2.56 × 10^3)	307_{sh} (2.52 × 10^3)	307_{sh} (2.48 × 10^3)
	393_{vs} (7.82 × 10^3)	393_{vs} (7.77 × 10^3)	393_{vs} (7.80 × 10^3)
	632_{vw} (1.72 × 10^2)	632_{vw} (1.70 × 10^2)	632_{vw} (1.40 × 10^2)

[a] Ratio of complex to H_2O_2; vs = very strong; s = strong; w = weak; vw = very weak; sh = shoulder; wsh = weak shoulder

Thermodynamic quantities for the interaction of H_2O_2 with [Ru(pdta–H)H_2O]

Table I lists the thermodynamic quantities associated with the interaction of [Ru^{III}(pdta–H)H_2O] with H_2O_2. The table also contains data for similar reactions of edta. It may be seen from the table that the values of the various equilibrium constants are almost the same for pdta and edta complexes; the complexes of pdta are more stable than those of edta on the basis of the former higher basicity. This is reflected in the enthalpy value of the protonation constant K_1 which is more positive for pdta than edta. The Ru^{III}(pdta)(H_2O) complex **2b** is therefore less susceptible to hydrolysis to form **2c** than the corresponding edta complex. Because of this factor, the second hydrolyses of the complexes to form dihydroxo species is not observed in pdta complexes. ΔG° values for the formation of complexes **2c** are almost the same for both ligands.

Interaction of complexes **1a** and **2a** with 0.5 equivalents of H_2O_2 gives Ru(III)-μ-hydroperoxo complexes. In these reactions the oxidation state of ruthenium remains +3. The enthalpy of the reaction (Table I) is highly favourable for the formation of μ-hydroperoxo complexes though the entropy term is fairly negative because of the associative nature of the reactions. The Ru(III)-pdta–μ-hydroperoxo complex is more stable than the corresponding edta complex.

Between a = 0–1 dissociation of a proton from the free carboxyl group of the ligand and after a = 1.0 the hydrolysis of the peroxo complexes to monohydroxo and dihydroxo species (except pdta are accompanied by large negative enthalpies and entropies.

Interaction of complexes **1a** and **2a** with 1.0 equivalents of H_2O_2 gives Ru(IV)–μ-peroxo complexes. The pdta complex is slightly more stable than the edta complex. The highly exothermic enthalpy ($\Delta H°$) values favour the formation of stable μ-peroxo complexes. The entropies have a large negative value, as observed for the formation of μ-peroxo complexes of cobalt.[10]

The large negative entropy values represent the loss of degrees of freedom of molecular O_2 in forming complexes. This trend is manifested even in the reaction with H_2O_2 to form the μ-peroxo complex, indicating that the source of O_2^{2-} is immaterial in the formation of dioxygen complexes. The dissociation of the carboxylate proton between a = 0–1 and the hydrolysis of corresponding complexes after a = 1.0 are all exothermic processes with large entropy values, as is the case for the Ru(III)–peroxo complexes.

It is of interest to compare the stability and thermodynamic parameters of μ-hydroperoxo and μ-peroxo complexes. The μ-hydroperoxo complexes are less stable and as expected have more endothermic enthalpies (about 2.6 kcal/mol)* than the μ-peroxo complexes. The difference in the entropy values is due to the higher oxidation state of the metal ion in the μ-peroxo complexes as compared to the μ-hydroperoxo complexes.

REFERENCES

1. M.M. Taqui Khan and A.E. Martell, "*Homogeneous Catalysis by Metal Complexes*," (Academic Press, New York, 1974), Vol. 1; T.G. Spiro, ed., "Metal Ion Activation of Dioxygen," (Plenum Press, New York, 1980); M.M. Taqui Khan, Plenary lecture: "Catalyzed Oxidation with Ruthenium(III) Dioxygen Complexes", 4th International Symposium on Homogeneous Catalysis, Leningrad, USSR, Sept., 1984; M.M. Taqui Khan, "*Advances in Homogeneous Catalysis*", (Pergamon Press, Oxford, 1986); M.M. Taqui Khan, *Oxid. Commun.*, **9**, 105 (1986); *Proc. Indian Natl. Sci. Acad.*, **52A** (1986); M.M. Taqui Khan and R.S. Shukla, *J. Mol. Catal.*, **44**, 85 (1988); **45**, 51 (1988); *Inorg. Chim. Acta*, 149 (1988).
2. M.M. Taqui Khan and G. Ramachandraiah, *Inorg. Chem.*, **21**, 2109 (1982); M.M. Taqui Khan, *Pure Appl. Chem.*, **55**, 159 (1983); M.M. Taqui Khan, A. Hussain, K. Venkatasubramanian, G. Ramachandraiah and V. Oomen, *J. Mol. Catal.*, **44**, 117 (1988).
3. M.M. Taqui Khan, A. Hussain, G. Ramachandraiah and M.A. Moiz, *Inorg. Chem.*, **25**, 3023 (1986).
4. R.J. Motekaitis and A.E. Martell, *Can. J. Chem.*, **60**, 168 (1982); **60**, 2403 (1982).
5. A.A. Diamantis and J.V. Dubrawski, *Inorg. Chem.*, **20**, 1142 (1981).
6. Unpublished results.
7. E.E. Mercer and R.R. Buckley, *Inorg. Chem.*, **4**, 1692 (1965); J.F. Endicott and H. Taube, *ibid.*, **4**, 437 (1965); M.M. Taqui Khan and G. Ramachandraiah, *Indian J. Chem., Sec. A*, **21A**, 41 (1982); K Shimizu, T. Matsubara and G.P. Saito, *Bull. Chem. Soc. Jpn.*, **47**, 1651 (1974).
8. Unpublished results.

---

* 1 cal = 4.18 J.

9. G. McLendon and A.E. Martell, *Coord. Chem. Rev.*, **19**, 1 (1976); A.B.P. Lever and H.B. Gray, *Acc. Chem. Res.*, **11**, 348 (1978).
10. H.K.J. Powell and G.H. Nancollas, *J. Am. Chem. Soc.*, **94**, 2664 (1972); G. McLendon and A.E. Martell, *J. Coord. Chem.*, **4**, 235 (1975); W.R. Harris, J.H. Timmons and A.E. Martell, *ibid.*, **8**, 251 (1979); G. McLendon and A.E. Martell, *J. Chem. Soc., Chem. Comm.*, 223 (1975); W.R. Harris, I. Murase, J.H. Timmons and A.E. Martell, *Inorg. Chem.*, **17**, 889 (1978); **21**, 1525 (1982).